ARMA/USRMS 05-881

Modeling Block Cave Subsidence at the Molycorp, Inc., Questa Mine—A Case Study

Gilbride, L. J.
Agapito Associates, Inc., Grand Junction, Colorado, USA
Free, K. S.
Agapito Associates, Inc., Grand Junction, Colorado, USA
Kehrman, R.
Molycorp, Inc., Questa, New Mexico, USA

This paper was prepared for presentation at Alaska Rocks 2005, The 40th U.S. Symposium on Rock Mechanics (USRMS): Rock Mechanics for Energy, Mineral and Infrastructure Development in the Northern Regions, held in Anchorage, Alaska, June 25-29, 2005.

ABSTRACT: The evolution of surface subsidence is an important focus of study above Molycorp, Inc.'s newest block cave at the Questa molybdenum mine near Taos, New Mexico. The case study compares mature glory hole subsidence over the Goathill Orebody and subsidence emerging in its earliest stage over the new D Orebody block cave. Subsidence above the D Orebody was first detected in April 2003, 30 months after caving was initiated. Caving propagated to surface through 550 m of overburden at an average rate of 0.21 m per day. At the end of 2004, an average of 100 m of draw over a 1.4-hectare (ha) block produced a near-circular subsidence basin 5.8 m deep at its center and 90 m offset from the center of the block. Observations to date indicate a cave ratio of 10:1 and a gross cave bulking factor on the order of 10%. Historically, cave-angle projection models have been used to predict subsidence extents for reclamation planning. In light of evolving regulatory concerns, efforts are underway to develop a more accurate subsidence predictor using a three-dimensional (3D) numerical model. Particle Flow Code (PFC3D), a discontinuum "ball" code, was selected for modeling because of its ability to simulate stress fracturing of the rock mass and large-scale mass flow underground and at the surface, which are believed to be the dominant physical phenomena governing the formation of block cave subsidence. Advances simulating subsidence in the Goathill and D orebodies with PFC3D are discussed.

1. INTRODUCTION

The Molycorp, Inc. (Molycorp), Questa block caving mine is located near the northern New Mexico town of Questa, as shown in Figure 1. Molybdenum has been mined at Questa for over 80 years. Molycorp began large-scale open pit mining in 1965, but by the mid-1970s, plans for underground mining were developed to combat high stripping ratios. By the end of 1976, a substantial high-grade deposit was delineated by exploratory drilling southwest of the open pit. The block caving method was selected because of the well-fractured nature of the rock mass, and the size and shape of the deposit [1]. Figure 2 shows the general layout of the current underground mine and the two main block caves: (1) the 300-m-deep Goathill Orebody and (2) the 600- to 800-m-deep D Orebody.

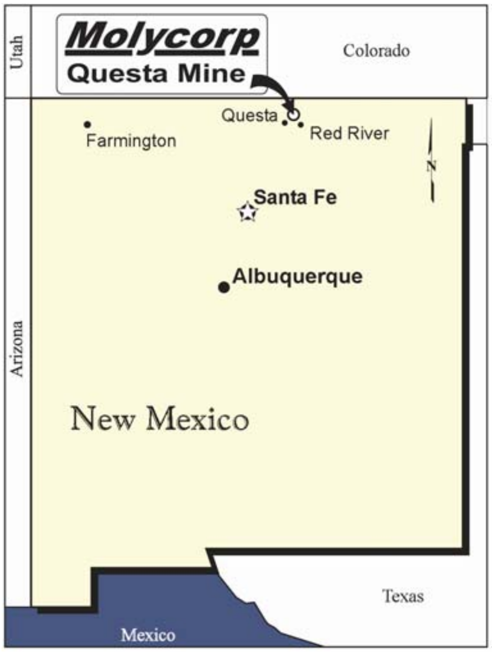

Figure 1. Location of Molycorp, Inc., Questa Mine

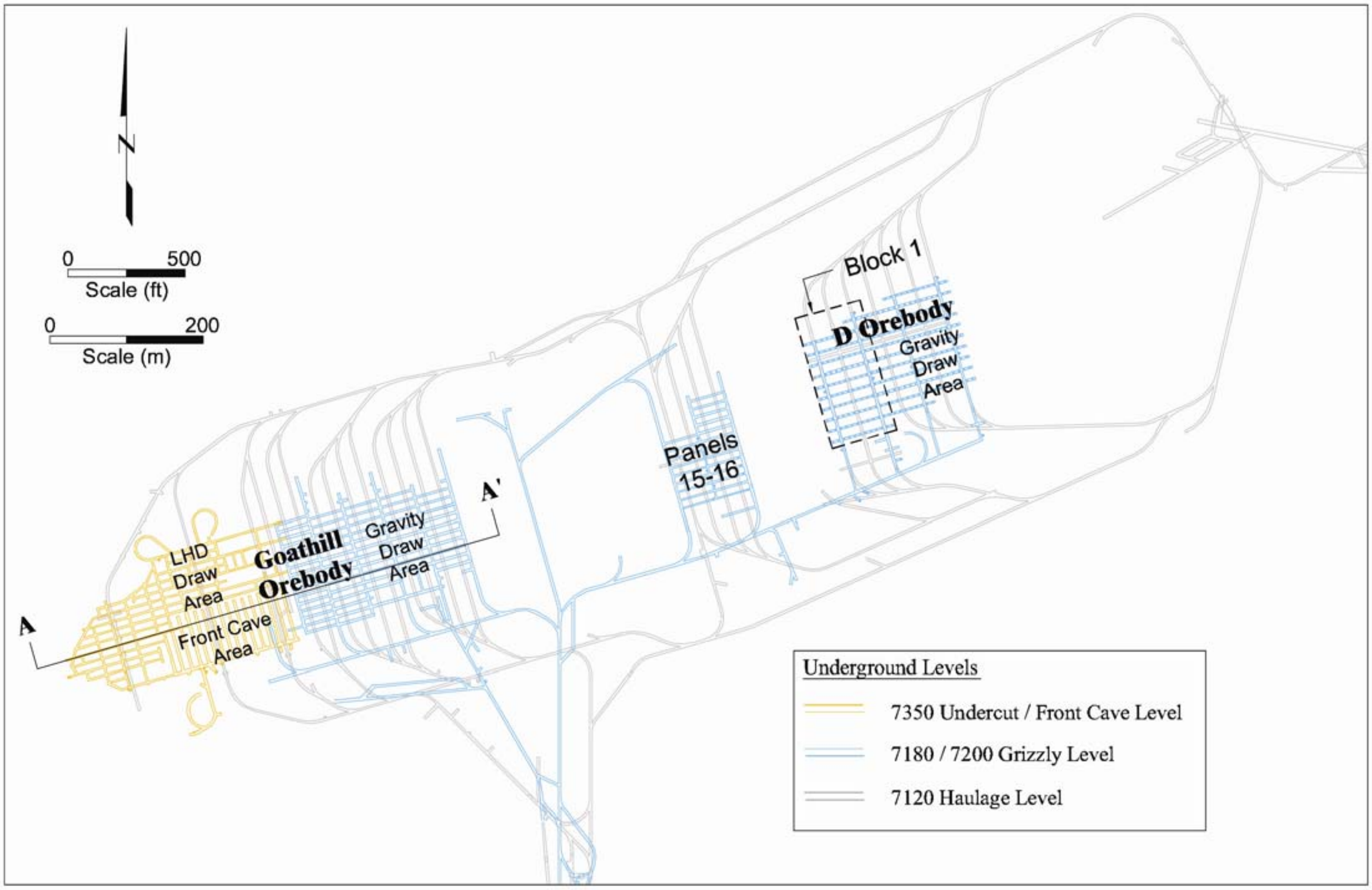

Figure 2. Plan View Mine Layout

Underground development began in 1979, followed by initial production in 1983 from the Goathill Orebody using the gravity draw method. Production peaked in the mid-1980s, reaching 16,000 tonnes per day. By 1992, the mine was placed in standby mode in response to declining molybdenum prices.

The mine was reactivated in 1995 and caving operations in the Goathill Orebody were converted from manual gravity draw to highly-mechanized, load-haul-dump (LHD) draw. In 1998, front caving, a variant of LHD mining, was attempted for 2 years. The front caving block pulled ore from the southern boundary of the original gravity cave. The individual gravity, LHD, and front caves were adjacent to one another and coalesced to form one single cave responsible for the formation of the Goathill glory hole shown in Figure 3. Mining was complete in the Goathill Orebody in 2000 when production shifted to the D Orebody.

Figure 3. Center of Goathill Glory Hole in 2004 (view to southwest)

Molycorp reverted to the original and proven gravity draw system in the D Orebody (Figure 4), which was favored for better ground control, cave fragmentation, and lower ventilation requirements [2]. The D Orebody comprises three sub-zones: D, Deep D, and Vein. The D sub-zone is divided into Blocks 1, 2, and 3. Caving was initiated in Block 1 in October 2000 and is the only part of the D Orebody in production as of February 2005. A total of 3.3 million tonnes have been produced by gravity draw from Block 1 as of the end of 2004.

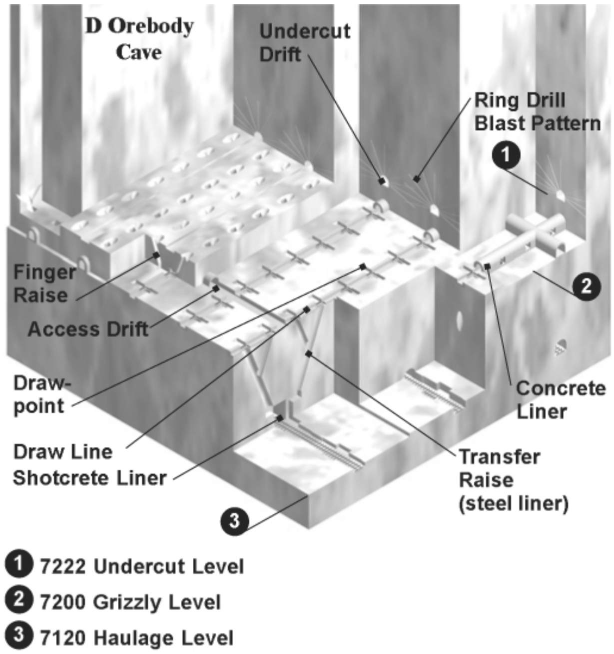

Figure 4. Gravity Draw System

Surface subsidence is a key concern for eventual mine closure and reclamation. In the past, conventional cave-angle projection models have provided reasonable estimates of the areal extents of subsidence for reclamation planning. In light of changing regulatory concerns, Molycorp recently invested in more sophisticated numerical modeling to improve the accuracy and precision of subsidence predictions. Leading this effort is the development of a 3D discontinuum caving and subsidence model utilizing PFC3D [3]. PFC3D shows considerable promise in its ability to simulate the principal mechanisms of caving and subsidence, and to replicate the historical subsidence behavior at the Questa Mine.

This paper discusses historical subsidence above the Goathill Orebody as an example of mature glory hole subsidence, followed by a discussion of subsidence in its earliest stage above the D Orebody. The cases represent the two extremes of subsidence for the Questa Mine and serve as valuable calibrators for modeling. Lastly, the paper describes efforts to model subsidence in both orebodies using the cave-angle method and PFC3D.

2. GOATHILL OREBODY SUBSIDENCE

2.1. *Production History*

Undercut levels in the Goathill Orebody ranged in depth between 260 and 365 m. Between 130 and 190 m of ore were ultimately drawn, constituting between 40% and 63% of the total overburden column, as illustrated in cross section in Figure 5. The ultimate extraction footprint measured approximately 5.3 ha. Total production from Goathill is summarized as follows:

Block	Total Production (million tonnes)
Gravity	16.0
LHD	5.5
Front Cave	0.2
TOTAL	21.7

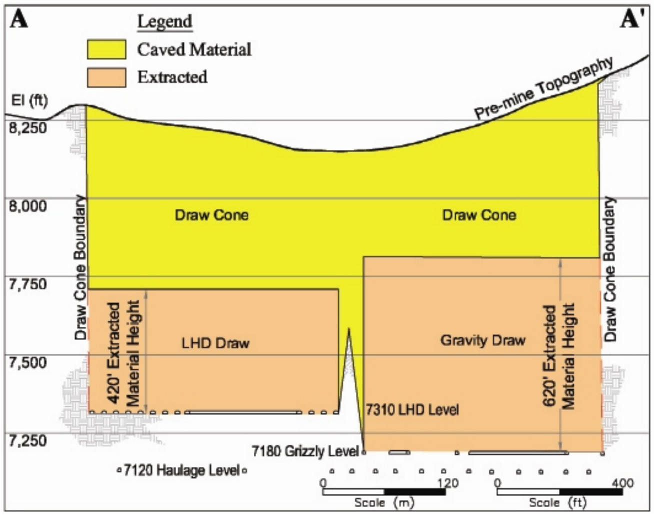

Figure 5. Goathill Orebody Cross Section

2.2. *Subsidence Characteristics*

Block caving subsidence is typically characterized by two zones of surface disturbance: (1) a primary subsidence zone, i.e., the “glory hole,” and (2) a secondary subsidence, or “relaxation zone,” peripheral to the primary subsidence zone. The primary subsidence zone is characterized by mass movement on the order of tens to hundreds of feet, while only moderate ground movement, on the order of tens of inches, is characteristic of the relaxation zone. Within the relaxation zone, subsidence can include visually discernable effects such as tension cracks, scarps, tilting, sliding, and damage to vegetation. Demarcation between the zones is oftentimes obvious on the ground and is normally taken to be the precipice of the glory hole.

The limits of the Goathill glory hole and relaxation zone in 2004 are shown in Figure 6.

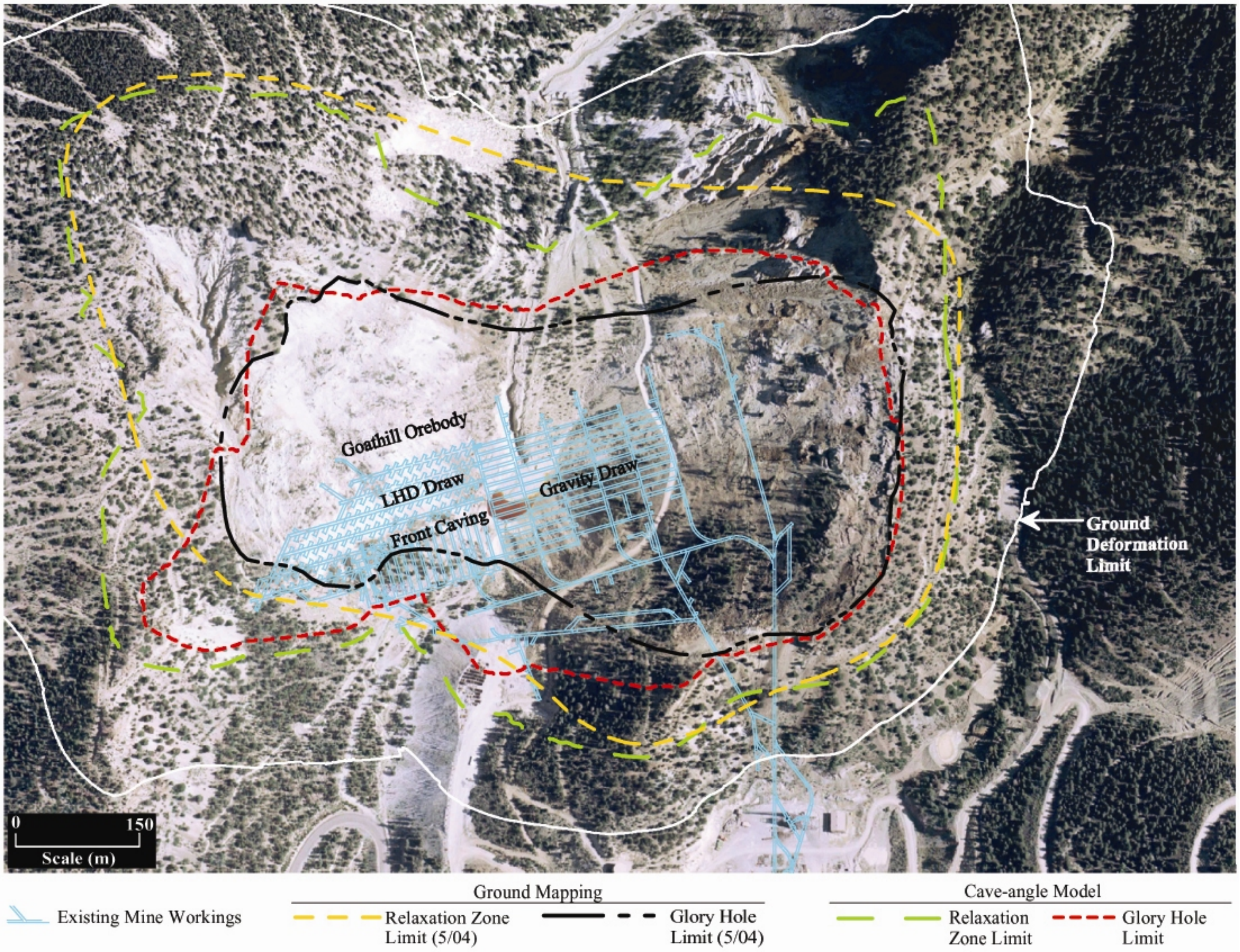

Figure 6. 2003 Aerial Photograph of Goathill Glory Hole and Subsidence Limits

The limits are based on (1) ground mapping and (2) detailed study of aerial photographs. The extents of the Goathill subsidence zones in May 2004 are summarized as follows:

Subsidence Zone	Total Area (ha)	Perimeter (m)
Glory Hole	29.5	2,365
Relaxation Zone	34.4	3,150

Cave angles (measured from horizontal at the edge of the undercut to the edge of surface cracking) range from 70° to 85° based on the 2004 subsidence extents. Relaxation angles (measured from horizontal at the edge of the undercut to the outer limits of relaxation features on surface) range from 51° to 84°. The volumetric difference between the total underground extraction (8.2 million cubic meters) and volume of the glory hole (4.7 million cubic meters) indicates a gross cave bulking factor between 9% and 21%, assuming that the zone of bulking is defined by cave angles ranging between 70° and 85°.

The glory hole continues to grow gradually by mass wasting along its periphery. An area encompassing approximately 14.2 ha on the eastern wall of the glory hole shows evidence of large-scale sliding. Slide features include escarpments, fresh cracks, block toppling, surface rubblization, tree tilting, and disturbance to hillside vegetation (Figure 7). While no subsurface measurements of movement exist, the gross surface expression of the east wall slide suggests that the slide is relatively shallow-seated (<60 m deep) and is occurring along a planar or near-planar surface.

Sliding is also evident on the northwest wall at the base of Goat Hill. Sliding originally occurred

Figure 7. Goathill Glory Hole East Wall Slide (view to east)

along a high-angle, southeast-dipping fault in mid-1997, forming a large headscarp. The headscarp currently measures more than 60 m tall. The slide and headscarp are shown in Figure 8. Structural mapping in the area suggests that similar, parallel structures exist uphill from the existing headscarp and that fault-controlled sliding will likely progress further up Goat Hill in the future. Future subsidence resulting from cave consolidation is likely to be partly obscured by erosion and sedimentation in the glory hole.

Figure 8. Goathill Glory Hole Goat Hill Slide (view to northwest)

3. D OREBODY SUBSIDENCE

3.1. Production History

The D Orebody Block 1 undercut ranges in depth between 550 and 670 m. The ore column ranges in height between 90 and 200 m, comprising between 16% and 37% of the total overburden column. As of the end of 2004, 50% of the ore column, or 100 m on average, was extracted in Block 1 over an area measuring 1.3 ha.

3.2. Subsidence Characteristics

Subsidence was first discovered in the form of surface tension cracks on the steep west-facing hillside above Block 1 in April 2003, approximately 900 days after the initiation of caving. By July 2004, a grid of 142 survey monuments was established for monitoring ground movement. By August 2004, the survey grid was expanded to 303 points to capture far-field movement. Surveys were conducted approximately every 2 months.

Subsidence at the end of 2004 is described by the map in Figure 9. Contours of (vertical) subsidence and horizontal displacement vectors are shown on the map relative to the underground workings. Salient features are summarized as follows:

- Maximum measured subsidence reached 5.8 m since monitoring began in July 2003. An additional 3 m or more of subsidence likely occurred prior to monitoring based on the scale of surface tension cracking at the time of discovery.
- The center of subsidence focused at a point approximately 90 m to the north-northwest of the center of Block 1 and 15 m past the north boundary of the Block 1 undercut. Horizontal deviation from the center of draw is attributed to local faulting.
- Maximum measured horizontal movement reached 4.6 m. Maximum horizontal movement focused immediately to the east and uphill from the center of subsidence.
- The average rate of subsidence at the center of subsidence was 1.43 cm per day (43.0 cm per month).
- The average rate of horizontal movement at the point of maximum horizontal movement was 1.13 cm per day (34.1 cm per month).
- The rate of surface subsidence showed no apparent correlation with fluctuations in the draw rate.

Based on the timing of the breakthrough of the cave to surface, Block 1 exhibits (1) an average cave ratio of 10:1 (height of cave line:height of drawn ore column), (2) a cave bulking factor of 10% or slightly less, and (3) a cave propagation rate on the order of 0.6 m per day. These

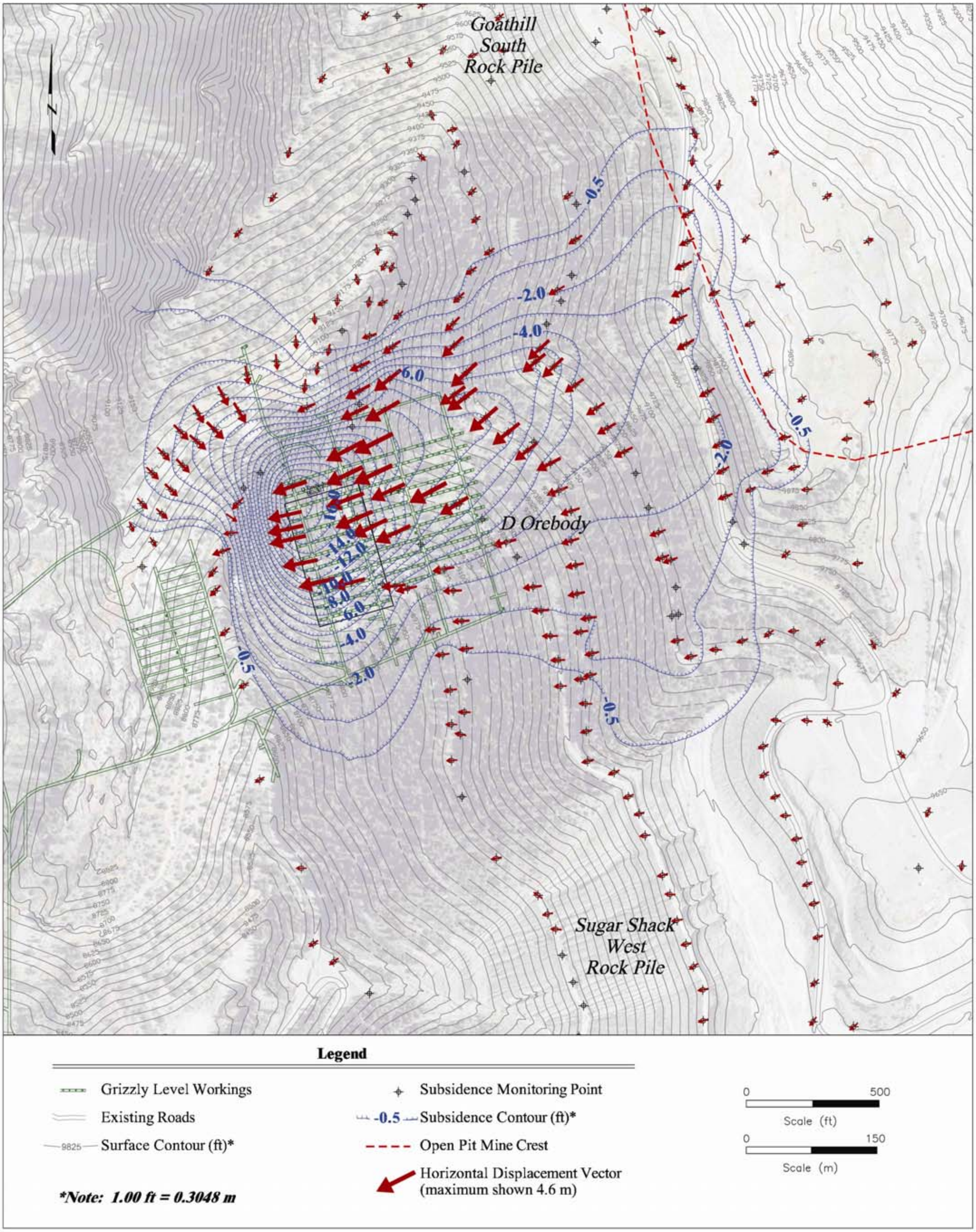

Figure 9. D Orebody Surveyed Subsidence Map—October 2004

characteristics correlate with values reported at other western U.S. caving operations:

Mine	Bulking Factor	Cave Rate (m/day)	Reference
San Manuel (South)	8.9%	0.49	[4]
Lakeshore	9.5%	1.98	[5]
Henderson	9.5%	0.70	[6]

As of the end of 2004, the Block 1 cave was too immature to define the ultimate cave or relaxation angles. Early subsidence, reaching as far as 550 m away from the undercut boundary of Block 1, suggests that relaxation angles will vary locally over a range between about 55° and 85°.

3.3. Hillside Movement

Subsidence over Block 1 initiated large-scale sliding of the west-facing hillside above the D Orebody some time in early 2003. By the end of 2004, the hillside above Block 1 has moved on the order of several feet to the west into the emerging subsidence basin. As much as 1.5 m of total movement has been measured since July 2003 near the top of the slide, located approximately 460 m east of Block 1. The rate of movement averaged about 0.30 cm per day (10.1 cm per month) in 2004. Tensile cracks at the top of the ridge continue to grow with sliding. Three boreholes were drilled and instrumented with time-domain-reflectometry (TDR) cables and inclinometers/extensometers in July 2004 to monitor slope movement as part of a separate study.

4. CAVE-ANGLE MODELING

By conventional practice, subsidence limits are estimated using cave-angle projections from the mining footprint to surface, as illustrated in Figure 10. For most mines, caving typically propagates upward from the extraction level through the rock mass at angles ranging from 75° to 90° from horizontal [7]. Numerical modeling and field observations suggests that a cave angle of 85° best represents conditions in the Goathill and D orebodies. Within this cone, the depth of subsidence at the surface is controlled by the gross swell factor within the cave.

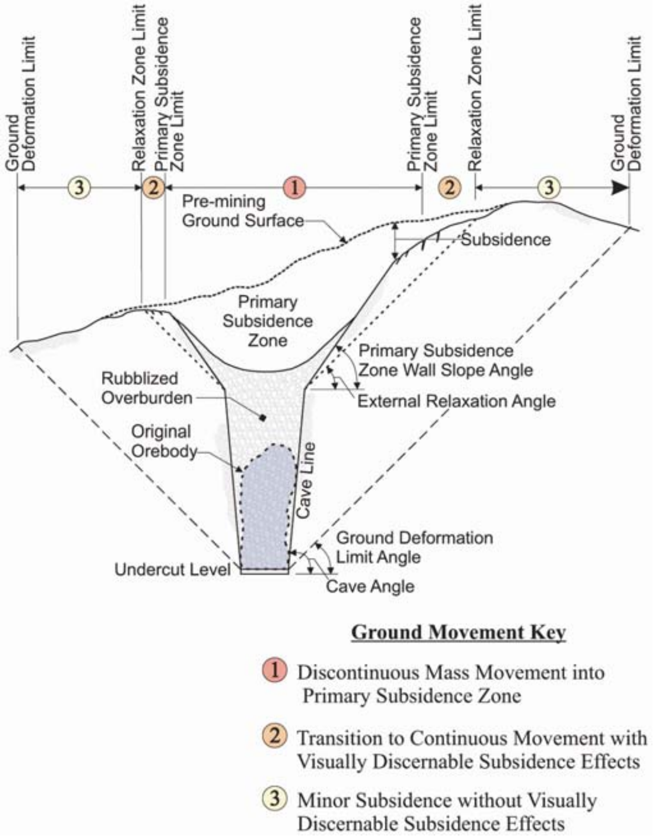

Figure 10. Cave-angle Subsidence Model

Considering a 10% swell factor and an ultimate draw of 190 m of ore in Block 1, the original ground surface is predicted to move downward as much as 150 m. However, the actual depth of the primary subsidence zone is expected to be significantly less because of mass wasting and natural infilling of the glory hole, as evidenced by the relatively shallow 60-m-deep glory hole at Goathill.

The ultimate angle of the primary subsidence basin walls depend upon the in situ and residual strength of the host rock and the steepness of the surrounding natural slopes. Good agreement with the glory hole geometry at Goathill was achieved using an 85° average cave angle and a 55° primary subsidence basin sidewall angle for estimating the limit of the glory hole (Figure 10). A 45° relaxation angle, suggested by Nickson et al. [8], proved realistic for describing the limit of the relaxation zone. Figure 6 shows reasonable agreement between the results of the cave-angle model and field mapping. Some deviation occurs on the northeast and southwest boundaries where a combination of sharp corners in the mine layout and steep topography causes the model to project unusually far beyond the actual limit of surface disturbance.

The limit of ground deformation shown in Figure 6 represents the farthest extent of mining-induced ground movement. Ground strain beyond this limit is not expected to be of sufficient magnitude to damage most mining and civil structures, such as buildings, roadways, and shafts. A 45° angle is generally adopted for conservative design [9] and was used for the original design at the Questa Mine.

The cave-angle model represents a simple, but effective predictive tool. The model, calibrated to conditions at Goathill, is considered a reasonably accurate general predictor of ultimate subsidence above the D Orebody. However, as a geometric construct, the cave-angle model is limited in its simplicity and ability to consider potentially important effects, including variable geology, local structure, ground stress, draw sequence, irregular caving geometries, and less-than-fully-developed glory hole subsidence. PFC3D was adopted for advanced modeling because of the code's ability to simulate these and other effects.

5. DISCONTINUUM MODELING

PFC3D is a 3D computer model capable of simulating continuum- and discontinuum-type ground deformation in response to mining. The host rock mass is represented as a bonded assemblage of rigid spheres. Elastic deformation of the rock mass is controlled by the elastic properties of the bonds. In the event of excess stress, bonds are capable of rupturing, allowing the process of rock mass fracturing and disintegration, and large-scale deformation and material flow, to be simulated. This ability makes PFC3D and other "ball" codes ideally suited for simulating caving mechanics and subsidence associated with block caving. A variety of investigators have made advances applying ball codes to subsurface caving mechanics [10, 11, 12, 13].

While ball codes have enormous potential, geomechanics modelers are faced with the sometimes controversial task of specifying model properties that have no direct physical analog and cannot be measured in the laboratory. Typically, this involves quantifying "artificial" properties on a micro-scale to produce a desired response on a macro-scale. For this reason, ball models are jointly considered phenomenological, where certain physical phenomena are explicitly simulated, and empirical, where abstract functions are calibrated to known responses to predicted behavior.

For subsidence modeling, numerous iterations were require to achieve the desired Hoek-Brown constitutive behavior of the rock mass prior to any attempt to simulate block caving. With a working constitutive model, it was possible to calibrate other "artificial" parameters influential to subsurface mass flow and subsidence.

5.1. Rock Mass Properties

Rock mass properties were assigned spatially according to a 3D block model developed by Molycorp from surface/underground geologic mapping and drill hole data. Blocks were assigned lithology and a geostatistically estimated RQD value. A 3D perspective of the RQD model above Block 1 in the D Orebody is shown in Figure 11.

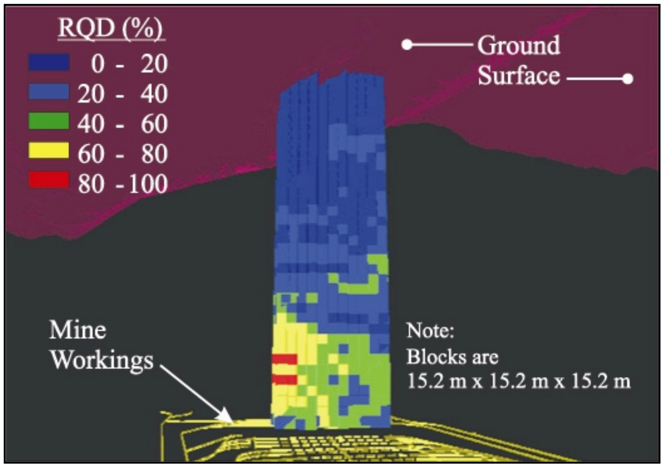

Figure 11. RQD Block Model—D Orebody Block 1

For modeling purposes, the complex geology of the Questa Mine was simplified to four predominant rock types: andesite, felsic dikes, intermediate dikes, and aplite-porphyry rocks. Rock quality at Questa is substantially affected by intense, but variable fracturing spaced as closely as 30 mm. Extensive mapping at the mine shows a range in Q [14] values from 0.002 to 8, which rates the rock mass from "exceptionally poor" to "fair" [15]. Rock mass properties were estimated according to the Geological Strength Index (GSI)

Table 1. Rock Mass Properties

Material		*GSI*	Young's Modulus (MPa)	Poisson's Ratio	Friction Angle (degrees)	Cohesion (MPa)	Rock Mass Strength (MPa)
Rock Type	RQD (%)						
Andesite	0 to 20	9	952	0.30	28.2	1.4	4.5
	20 to 40	19	1683	0.30	33.1	2.0	7.4
	40 to 60	24	2193	0.30	35.2	2.4	9.1
	60 to 80	27	2611	0.30	36.7	2.9	11.7
	80 to 100	29	2974	0.30	37.4	3.0	12.3
Felsic Dikes	0 to 20	9	952	0.30	28.2	1.1	3.6
	20 to 40	19	1683	0.30	33.1	1.6	5.9
	40 to 60	24	2193	0.30	35.2	1.9	7.3
	60 to 80	27	2611	0.30	36.7	2.4	9.4
	80 to 100	29	2974	0.30	37.4	2.4	9.8
Intermediate Dikes	0 to 20	9	952	0.30	28.2	1.6	5.4
	20 to 40	19	1683	0.30	33.1	2.4	8.0
	40 to 60	24	2193	0.30	35.2	2.8	11.0
	60 to 80	27	2611	0.30	36.7	3.5	14.1
	80 to 100	29	2974	0.30	37.4	3.6	14.7
Aplite	0 to 20	9	952	0.30	28.2	1.9	6.3
	20 to 40	19	1683	0.30	33.1	2.8	10.3
	40 to 60	24	2193	0.30	35.2	3.3	12.8
	60 to 80	27	2611	0.30	36.7	4.1	16.4
	80 to 100	29	2974	0.30	37.4	4.2	17.2

introduced by Hoek et al. [16] and are summarized in Table 1 according to RQD.

Rock mass properties in Table 1 were translated to micro-properties in PFC3D by reproducing the desired Hoek-Brown properties in synthetic triaxial tests in PFC3D. Triaxial "tests" were conducted at confining pressures up to 21 MPa corresponding to stress conditions in the block cave. Because the properties are highly dependent upon ball diameter, triaxial tests were performed at the same ball size used in the mine-scale models.

The triaxial geometry and a typical model stress-strain curve are shown in Figure 12. Planar octagon symbols in the figure represent individual bond fractures or "micro-cracks" which ultimately govern failure. Testing was repeated with adjustments to model micro-parameters until a satisfactory replication of the Hoek-Brown strength envelope and elastic modulus was achieved. Although many "artificial" micro-parameters exist within PFC3D, calibration was ultimately limited to the following micro-parameters which were determined to dominate the strength and stiffness response of the rock mass:

- Bond elastic modulus, E_c
- Bond normal to shear stiffness ratio, k_n/k_s
- Bond normal strength, s
- Bond shear strength, t

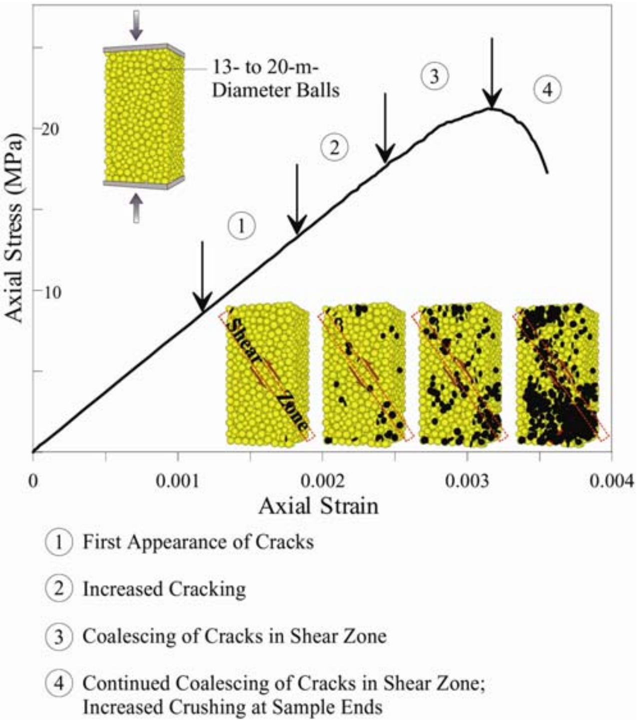

Figure 12. Synthetic Rock Mass Triaxial Test

5.2. Model Geometry and Mining Sequence

Separate models were constructed for the Goathill and D orebodies. Figure 13 illustrates the geometry of the Goathill model. Color banding is shown in the figure as a visual aid to highlight the variable surface topography. The volumetric extents of the models and mesh resolution, i.e., ball size, were practically constrained by computational run time. Every effort was made to limit the volume of the models so that ball diameters could be made as small as possible in the belief that smaller-diameter balls add more degrees of freedom and the ability to simulate smaller-scale phenomena, thus affording better accuracy. Ultimately, it proved necessary to limit the models to a maximum of 125,000 balls with diameters ranging from 13 to 20 m. Model run-times averaged 15 to 20 days on a Pentium 4, 2.4-GHz personal computer.

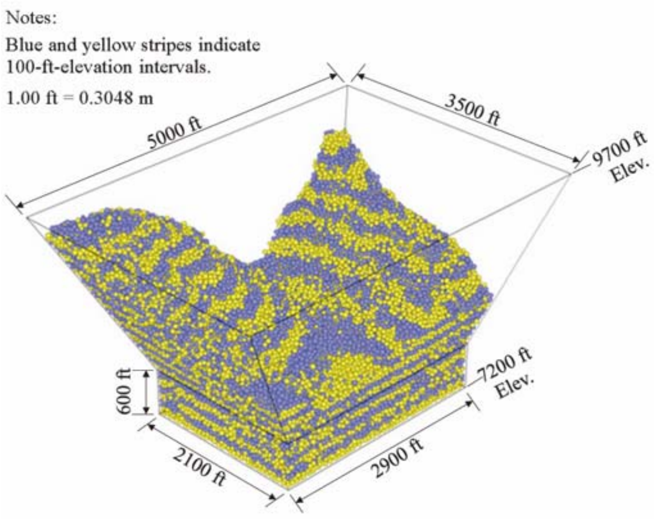

Figure 13. Goathill Orebody Subsidence Model

The undercut levels defined the base elevations of the models. Draw was simulated by eliminating balls at multiple, individual drawpoints at the base of the models. Balls were removed according to mine records in monthly steps to simulate the actual draw. Detailed records for individual draw windows were incorporated in the D Orebodymodel. The Goathill model assumed uniform draw per block because of less complete records; however the gravity, LHD, and front-cave blocks were mined in their historical sequence.

Balls drawn from the model initiated the step-wise process of stress redistribution, ball-to-ball bond fracturing, and mass movement into the void. A cross section of the D Orebody model in Figure 14 illustrates the pattern of mass movement resulting from complete draw of the ore column in Blocks 1–3. Mass flow in the cave is apparent by the disturbance of the originally horizontal color bands in part (a) of the figure. Displacement vectors of individual balls, shown in part (b) of the figure, highlight zones of active mass flow. The model indicates a stress-relaxation zone peripheral to the cave where ball-to-ball bonds are broken, but movement into the cave is retarded by frictional forces.

5.3. Model Results

Although the completeness of mine records prevented a direct comparison of the PFC3D model with the staged evolution of the Goathill glory hole, the model could be compared with several important features of the relatively mature Goathill glory hole in 2004. Figure 15 is a plan view of the PFC3D model surface. The epicenter of mass flow indicated by the area of peak downward movement of surface balls correlates with the center of the existing glory hole.

The model appears most accurate along the east-southeast wall of the glory hole where the glory hole edge coincides with the limits mapped in 2004. The model also indicates shallow-seated slope movement on this wall consistent with field observations. To the north and west, the model shows considerably more basement movement and hillside sliding into the glory hole than observed to date. The model predicted a final glory hole close in size to the much larger relaxation zone limit mapped in 2004, suggesting that rock mass strength is underestimated, at least near the surface, in the model.

Because the model does not account for time-dependent rock mass behavior, the model results represent long-term subsidence. Some potential exists for the glory hole to grow beyond its current limit and more closely resemble the model results. This appears imminent to the northwest along the base of Goat Hill where the base of Goat Hill is continuing to slide into the glory hole per the mechanism predicted in the model.

The same model properties used in the Goathill model were applied to the D Orebody, Block 1 model. While the Goathill model provided calibration with the large-scale features of late-stage surface subsidence, the D Orebody model

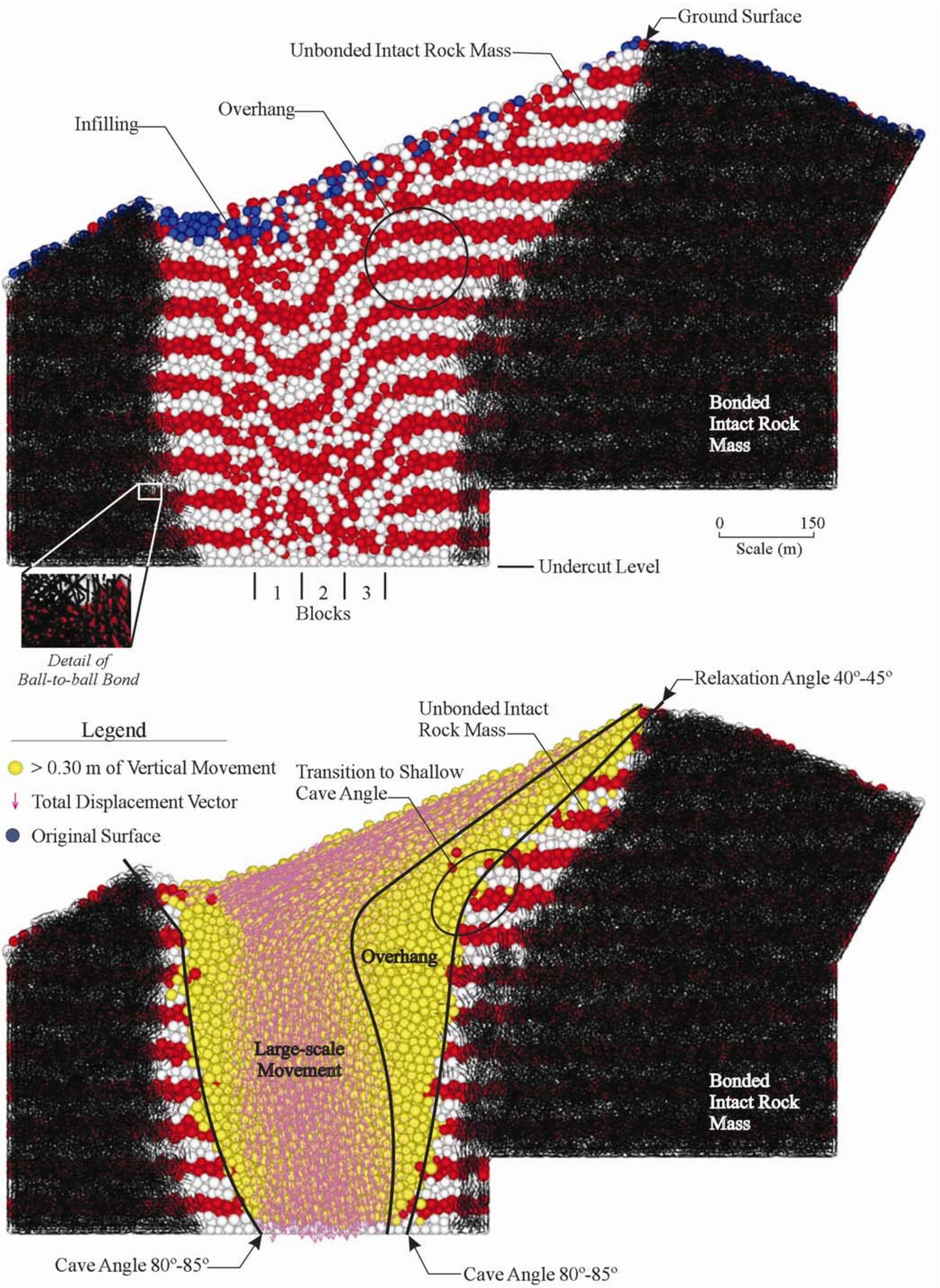

Figure 14. Cross Section of Subsidence Mass Movement from Block Caving—D Orebody Model

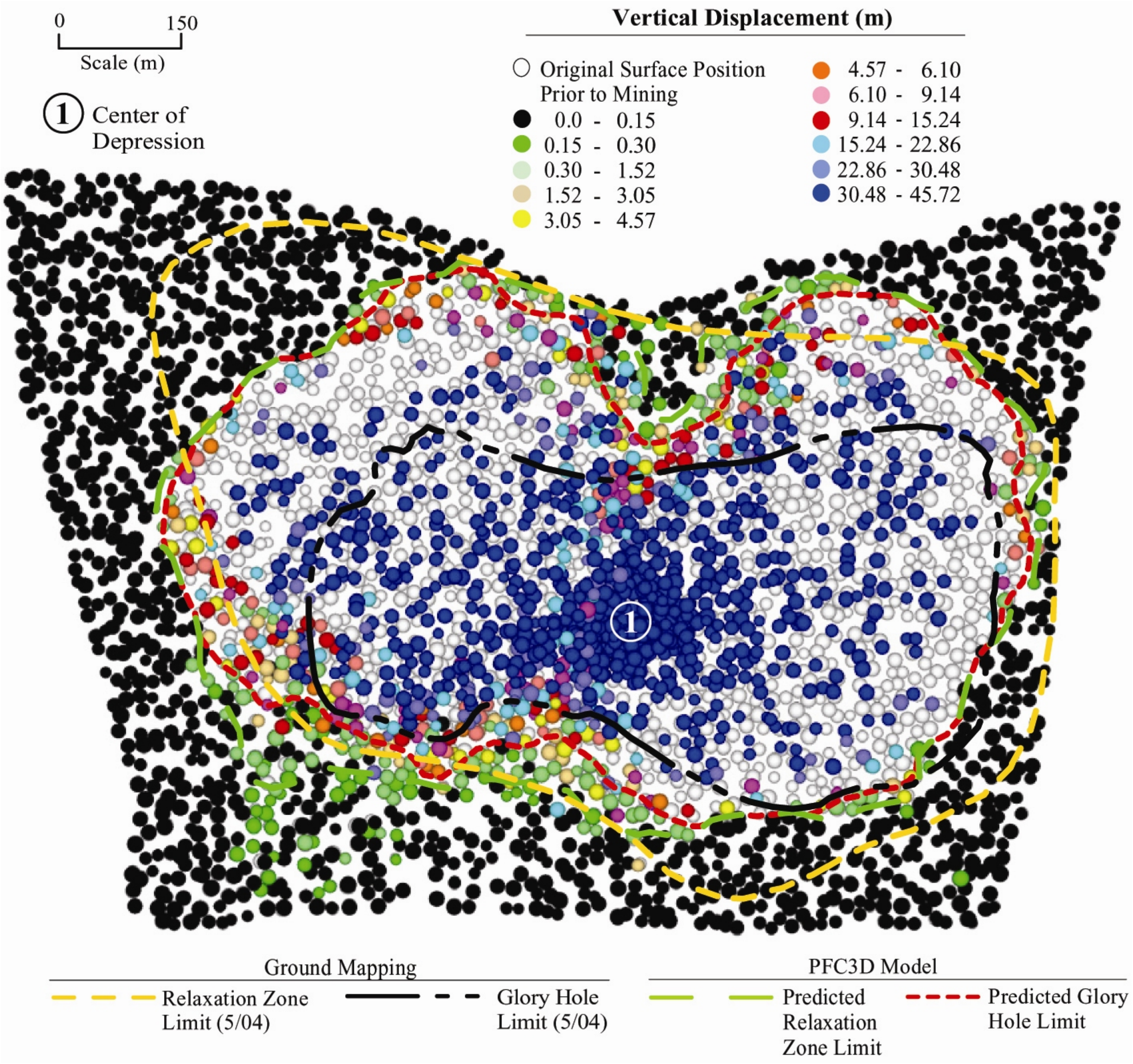

Figure 15. Plan View Map of Surface Movement and Subsidence Limits—Goathill Orebody Model

allowed model response to be calibrated with detailed chronological records of early-stage subsidence.

Figure 16 compares modeled and measured subsidence at the epicenter of the Block 1 subsidence basin since the beginning of surveying. The figure plots subsidence and subsidence rate against time. The plot shows that the PFC3D model lags the actual time that measurable subsidence began on surface by approximately 12 months. Because minor subsidence may have occurred prior to the first survey, the lag time may actually exceed 12 months.

The lag is attributed to a slow propagation of the cave to surface in the model. The large ball diameters showed resistance to small volumetric changes in the early stages of draw. Special provisions were made to decrease ball interface friction as a function of downward movement in the cave to accelerate cave propagation to surface, and to simulate the effects of comminution and densification. However, a friction angle less than about 5° promoted excessive lateral growth of the cave and could not maintain the relatively steep (80°–85°) cave angles thought to exist in practice.

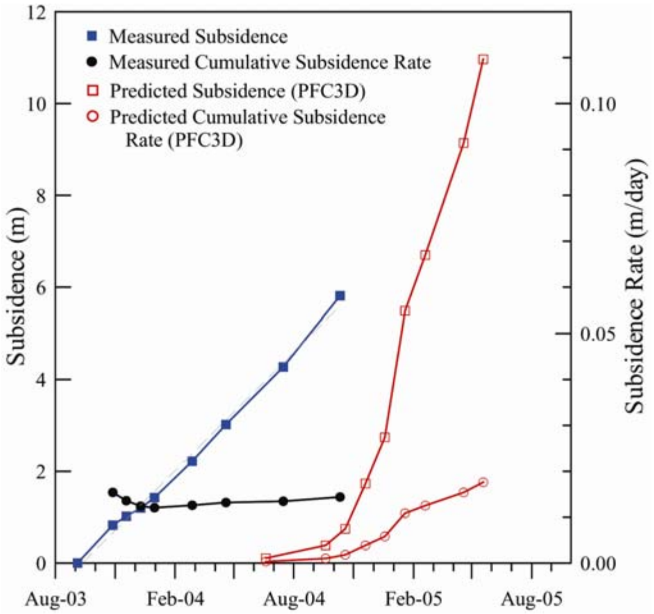

Figure 16. Modeled and Measured Subsidence Histories—D Orebody Block 1 Model

Once a large enough volume of ore was eventually drawn in the model, the "hang-up" of the large balls was overcome and caving progressed relatively smoothly. Figure 16 shows closure of the modeled-measured time lag and a trend toward the converging magnitudes and rates of subsidence in more recent months. Once the cave became more mature, the model was able to reproduce the observed 10% gross bulking factor in the cave.

6. CONCLUSIONS

Block caving subsidence is a complex combination of highly discontinuous rock mass flow surrounded by a zone of minor discontinuous/continuous ground relaxation. The true advantage of a ball code for modeling this type of environment lies in a ball code's ability to simulate large-displacement mass flow simultaneous with elastic- and small-strain, inelastic deformation. This capability offers enormous potential for advancing predictive accuracy.

However, as a state-of-the-art technology, ball codes are relatively immature and, before more universal favor is found, will continue to pose two types of important challenges to analysts. First is the usual practical challenge of achieving computational efficiency, i.e., fast model run-times with ball diameters small enough to ensure realistic behavior. Because the rock mass cannot disintegrate smaller than individual balls, the minimum ball size within the model will control the scale of physical phenomena that can be simulated.

Shortcomings of the Molycorp PFC3D models are attributed to the large ball diameters more so than any other model parameter. It is likely that the large diameters prevented some potentially influential smaller-scale deformation mechanisms from developing in the cave and near the surface. For this reason, and that material properties must be scaled to ball size, ball codes are inherently more "mesh dependent" than comparable continuum models. In the authors' experience with mine-scale subsidence models, a ball size that is "too small" has yet to be attained.

The other major challenge facing analysts is justification of the "artificial" properties required for ball code modeling. Although a concern, justification of these "artificial" parameters is expected to be forthcoming with research focused on sensitivity analysis of parameters at the macroscopic scale. Although the use of a ball code to simulate subsidence is substantially a pioneering effort, the model results are considered to be reasonably realistic and correlate surprisingly well with observed phenomena.

For subsidence modeling in the future, little question exists as to the value of ball code modeling; the challenge is in "coming to grips" with model predictions based exclusively on non-physical properties that can simulate real physical phenomena.

REFERENCES

1. Shoemaker, D. R. 1981. Method Selection at Questa. *Design and Operation of Caving and Sublevel Stoping Mines*. American Institute of Mining, Metallurgical, and Petroleum Engineers, Inc. New York.
2. Gilbride, L. J. and R. Kehrman. 2004. Ground Support Design Using Three-Dimensional Numerical Modeling at Molycorp, Inc.'s, Block Caving Questa Mine. *MassMin 2004—Proceedings*. Santiago, Chile. August 22–25, 2004. pp. 338–349.
3. Itasca Consulting Group, Inc. 2003. *PFC^{3D} User's Guide*. Minneapolis, Minnesota.
4. Johnson, G. H. and J. H. Soule. 1963. *Measurements of Surface Subsidence, San Manuel mine, Pinal County, Arizona*. Bureau of Mines Report of Investigations 6204.

5. Panek, L. A. 1984. *Subsidence in Undercut-Cave Operations, Subsidence Resulting from Limited Extraction of Two Neighboring-Cave Operations*. Department of Mining Engineering. Michigan Technological University. Houghton, Michigan.

6. Brumleve, C. and M. Maier. 1981. Applied Investigation of Rock Mass Response to Panel Caving, Henderson Mine, Colorado. *Design and Operation of Caving and Sublevel Caving Mines*. D. Steward, ed. SME of AIME. pp. 223–249.

7. Laubscher, D. H. 1990. A Geotechnical Classification System for the Rating of Rock Mass in Mine Design. *Journal of the South African Institute of Mining and Metallurgy*. October. 90(10): 257–273.

8. Nickson, S., A. Coulson, and J. Hussey. 2001. Noranda’s Approach to Evaluating a Competent Deposit for Caving. *Underground Mining Methods, Engineering Fundamentals and International Case Studies*. Edited by W. A. Hustrulid and R. L. Bullock. Society of Mining, Metallurgy and Exploration, Inc. Littleton, CO. pp. 521–534.

9. de la Vergne, J. N. 2003. *Hard Rock Miner’s Handbook*. 3rd Edition. McIntosh Engineering, Ltd. North Bay, Ontario, Canada. Section 2.2. p. 14.

10. Lorig, L. J. and P. A. Dundall 2000. A Rapid Gravity Flow Simulator. *Final Report, International Caving Study*. Ed: E. T. Brown. JKMRC and Itasca Consulting Group, Inc. Brisbane.

11. Brown, E. T. 2003. Block Caving Geomechanics. *The International Caving Study Stage I-1997 through 2000*. The University of Queensland, Australia.

12. Esterhuizen, G.S., L. Rachmad, A. V. Potapov, and L. K. Nordell. 2004. Investigation of Swell Factor in the Block Cave Draw Column. *MassMin 2004—Proceedings*. Santiago, Chile. August 22–25, 2004. pp. 215–219.

13. Selldén, H. and M. Pierce. 2004. PFC3D Modeling of Flow Behaviour in Sublevel Caving. *MassMin 2004—Proceedings*. Santiago, Chile. August 22–25, 2004. pp. 201–214.

14. Barton, N., R. Lien, and J. Lunde. 1977. Evaluation of Support Requirements for Underground Excavations. *Proceedings of the 16th U.S. Symposium of Rock Mechanics*.

15. Agapito, J. F. T. and D. R. Shoemaker. 1987. Ground Stability and Support in Block Caving Operations at Molycorp’s Questa Mine. *Proceedings of the 28th U.S. Symposium of Rock Mechanics*.

16. Hoek, E., P. K. Kaiser, and W. F. Bawden. 1995. *Support of Underground Excavations in Hard Rock*. A.A. Balkema. Netherlands.